Calculation of spin distribution for several fission reaction systems induced by nucleons and heavy ions

S. Soheyli* and M. Khamehchi
Bu-Ali Sina University, Department of Physics, Hamedan, Iran
(Received 22 April 2010; published 6 July 2010)

Compound nucleus spin distribution has been calculated for several fission reaction systems induced by nucleons and heavy ions. Determination of the spin distribution for these systems is based upon the comparison between the experimental data of the fission fragment angular distributions as well as the prediction of the standard saddle-point statistical model (SSPSM). For the systems, the two cases, namely with and without neutron emission corrections were considered. This method is used for the first time to determine compound nucleus spin distribution. Afterwards, our theoretical results have been compared with the data obtained from the coupled-channel technique as well as the Wong model, and satisfactory agreements were found. Furthermore, we have introduced a semiclassical approximation relation for the compound nucleus spin distribution of these systems.

DOI: 10.1103/PhysRevC.82.014605 PACS number(s): 25.70.Jj, 25.85.Ge, 27.80.+w, 27.90.+b

I. INTRODUCTION

Compound nucleus spin distribution is a crucial quantity in determining fusion-fission dynamics, although there has not been introduced any precise method to determine it. In this paper, to calculate compound nucleus spin distribution, two methods are presented. In the first method, the values of spin distribution for 20 induced-fission reaction systems are determined by the fission fragment angular distribution method. This method is based upon the comparison between the experimental data of the fission fragment angular distribution as well as the prediction of the standard saddle point statistical model (SSPSM). Calculation through this method is considered with and without neutron emission correction in the reactions. In the second method, there is presented an approximate method to determine compound nucleus spin distribution based upon quantum-classical relationships.

II. STANDARD SADDLE-POINT STATISTICAL MODEL

Fission fragment anisotropy A defined as

$$A = \frac{W(0^{\circ} \text{ or } 180^{\circ})}{W(90^{\circ})} \cong 1 + \frac{\langle I^2 \rangle}{4{K_0}^2}, \quad (1)$$

where $\langle I^2 \rangle$ is the mean-square angular momentum of the compound nucleus and ${K_0}^2$ represents the variance of the K Gaussian distribution [1]. The standard deviation of the K (Gaussian distribution) is given by

$$ {K_0}^2 = \frac{\Im_{\text{eff}} T}{\hbar^2} = \left(\frac{1}{\Im_{\parallel}} - \frac{1}{\Im_{\perp}} \right)^{-1} \frac{T}{\hbar^2}, \quad (2)$$

where $\Im_{\text{eff}}$, $\Im_{\parallel}$, $\Im_{\perp}$, and T are the effective moment of inertia, the moment of inertia parallel to the symmetry axis, the moment of inertia perpendicular to the symmetry axis, and the nuclear temperature at the saddle point, respectively. T, the nuclear temperature at the saddle point, can be calculated as

$$T = \sqrt{\frac{E_{ex}}{a}} = \sqrt{\frac{E_{\text{com}} + Q - B_f - E_R}{a}}, \quad (3)$$

where E_{ex} denotes the excitation energy of the compound nucleus, while E_{com}, Q, B_f, and E_R represent the projectile energy in the center-of-mass frame, the Q value, fission barrier height, and rotational energy of the compound nucleus, respectively. a stands for the level density parameter at the saddle point. In this paper, we have taken $a = \frac{A_{\text{C.N.}}}{9}$ MeV^{-1} where $A_{\text{C.N.}}$ is the mass number of compound nucleus.

Due to the use of the SSPSM, in the calculations, it is assumed that neutrons are emitted before the compound nucleus approaches the saddle point.

Excitation energy of compound nucleus considering neutron emitted in the fission process, is given by

$$E_{ex} = E_{\text{com}} + Q - B_f - E_R - \nu E_n, \quad (4)$$

where ν is the number of pre-fission neutrons, and E_n is the average energy of an emitted neutron. The energy carried by the neutron is assumed to be 5 MeV. Also, if the neutron energy is considered as $7 \leqslant E_n \leqslant 9$ MeV, the quantity of spin distribution varies at most by 2–4 % for each neutron emitted in this computation procedure. It is now clear that because of the hindrance to fission, a larger number of particles, neutrons in particular, are emitted from the fissioning system. These pre-fission neutrons are emitted not only during the transition stage up to the saddle point but also during the decent from the saddle to the scission point. The emission of neutrons before reaching the saddle point has the effect of lowering the available excitation energy at this point and this in turn will reduce the variance of the K distribution. In the present work, the pre-fission neutrons are taken to be emitted before the saddle point, since it is not straightforward to separate experimentally the contribution of neutrons emitted before the

*Corresponding author: soh@basu.ac.ir

TABLE I. Heavy-ion induced fission systems along with their compound nucleus.

Heavy-ion fission systems	Compound nucleus
$^{16}O + ^{232}Th$	^{248}Cf
$^{12}C + ^{236}U$	^{248}Cf
$^{11}B + ^{237}Np$	^{248}Cf
$^{32}S + ^{208}Pb$	^{240}Cf
$^{14}N + ^{232}Th$	^{246}Bk
$^{11}B + ^{235}U$	^{246}Bk
$^{11}B + ^{238}U$	^{249}Bk
$^{12}C + ^{232}Th$	^{244}Cm
$^{28}Si + ^{208}Pb$	^{236}Cm
$^{9}Be + ^{232}Th$	^{241}Pu
$^{24}Mg + ^{208}Pb$	^{232}Pu
$^{16}O + ^{209}Bi$	^{225}Pa
$^{19}F + ^{208}Pb$	^{227}Pa
$^{19}F + ^{232}Th$	^{251}Es
$^{12}C + ^{237}Np$	^{249}Es
$^{10}B + ^{232}Th$	^{242}Am
$^{16}O + ^{208}Pb$	^{224}Th
$^{19}F + ^{197}Au$	^{216}Ra

saddle point and the ones emitted after the saddle point but before the scission point.

III. FISSION FRAGMENT ANGULAR DISTRIBUTION METHOD

The calculation method is based upon the experimental data for the fission fragment angular distribution. In this method, the quantity $\langle I^2\rangle$ is considered as a linear equation in terms of the projectile energy in the center-of-mass framework [2], then, having found the values of B_f, E_R, and $\frac{\Im_{\rm eff}T}{\hbar^2}$ and using the experimental data for the angular anisotropy of fission fragments [3-12], we could obtain $\langle I^2\rangle$ by comparing the experimental data of angular anisotropy as well as the prediction of SSPSM. In the present work, we determined the values of $\langle I^2\rangle$ for 18 systems undergoing induced fission with heavy ion as well as those of two systems undergoing induced fission with nucleon. In Table I, the systems are listed along with their compound nucleus.

We take the relationships of $\langle I^2\rangle$ in terms of $\frac{E_{\rm com}}{V_b}$ as $\langle I^2\rangle = a_\nu \frac{E_{\rm com}}{V_b} + b_\nu$, where $\nu = 0, 1, 2$ denotes considering without the emission of neutron, emission of one neutron, emission of two neutrons, respectively, and V_b denotes the Coulomb barrier height. Table II shows a_ν and b_ν for the heavy-ion induced fission systems. Figures 1–6 show the compound nucleus spin distribution determined by fission fragment angular distribution method with and without neutron emission correction for the systems that formed similar Cf, Bk, Cm, Pu, Pa, and Es isotopes, respectively.

Figures 7–9 show the compound nucleus spin distribution determined by fission fragment angular distribution method with and without neutron emission correction for the $^{10}B + ^{232}Th$, $^{16}O + ^{208}Pb$, and $^{19}F + ^{197}Au$ systems, respectively. In the induced fission performed by light projectile such as proton, neutron, and α particle, we must pay attention to some important points expressing the difference between induced fission with light projectiles and heavy ion induced fission. In fission with light projectiles, the energy in the center-of-mass framework ($E_{\rm c.m.}$) is roughly the same as that in the laboratory framework. Due to the low weight of projectile, rotational energy (E_R) can be neglected. Given all necessary data including B_f and $\frac{\Im_{\rm eff}}{\hbar^2}$ [12], we can determine the compound

TABLE II. Coefficients of equation $\langle I^2\rangle$ in terms of $\frac{E_{\rm c.m.}}{V_b}$ without considering neutron emission and by considering the correction related to neutron emission.

Heavy-ion fission systems	$a_\circ$	$b_\circ$	a_1	b_1	a_2	b_2
$^{16}O + ^{232}Th$	3809.34	−3430.74	3642.98	−3297.52	3482.42	−3172.36
$^{12}C + ^{236}U$	2235.00	−2029.73	2182.25	−2007.43	2130.64	−1988.60
$^{11}B + ^{237}Np$	1596.06	−1508.09	1540.68	−1467.52	1486.31	−1429.41
$^{32}S + ^{208}Pb$	2521.15	−1964.83	2481.59	−1984.29	2444.85	−2007.43
$^{14}N + ^{232}Th$	2657.06	−2227.97	2557.06	−2157.98	2457.37	−2090.22
$^{11}B + ^{235}U$	819.12	−614.26	777.84	−592.14	738.85	−573.47
$^{11}B + ^{238}U$	909.02	−775.83	865.50	−723.77	790.06	−669.14
$^{12}C + ^{232}Th$	2520.80	−2411.03	2387.74	−2287.69	2249.77	−2160.82
$^{28}Si + ^{208}Pb$	4085.20	−3241.52	4025.92	−3280.27	3970.31	−3325.17
$^{9}Be + ^{232}Th$	1500.67	−1468.21	1405.45	−1377.69	1308.18	−1286.01
$^{24}Mg + ^{208}Pb$	2822.95	−2082.23	2770.82	−2073.60	2719.75	−2066.83
$^{16}O + ^{209}Bi$	5142.16	−5118.57	4877.85	−4846.12	4624.32	−4856.34
$^{19}F + ^{208}Pb$	1392.71	−1047.92	1378.15	−1093.43	1364.73	−1141.22
$^{19}F + ^{232}Th$	4537.96	−3991.86	4300.21	−3790.51	4064.60	−3592.93
$^{12}C + ^{237}Np$	2365.57	−2299.27	2253.64	−2196.80	2138.83	−2092.64
$^{10}B + ^{232}Th$	2206.54	−2259.43	2082.98	−2133.75	1957.33	−2006.37
$^{16}O + ^{208}Pb$	3658.66	−3269.54	3448.57	−3088.14	3248.61	−2917.98
$^{19}F + ^{197}Au$	7361.20	−6450.38	6885.97	−6046.81	6430.95	−5666.81

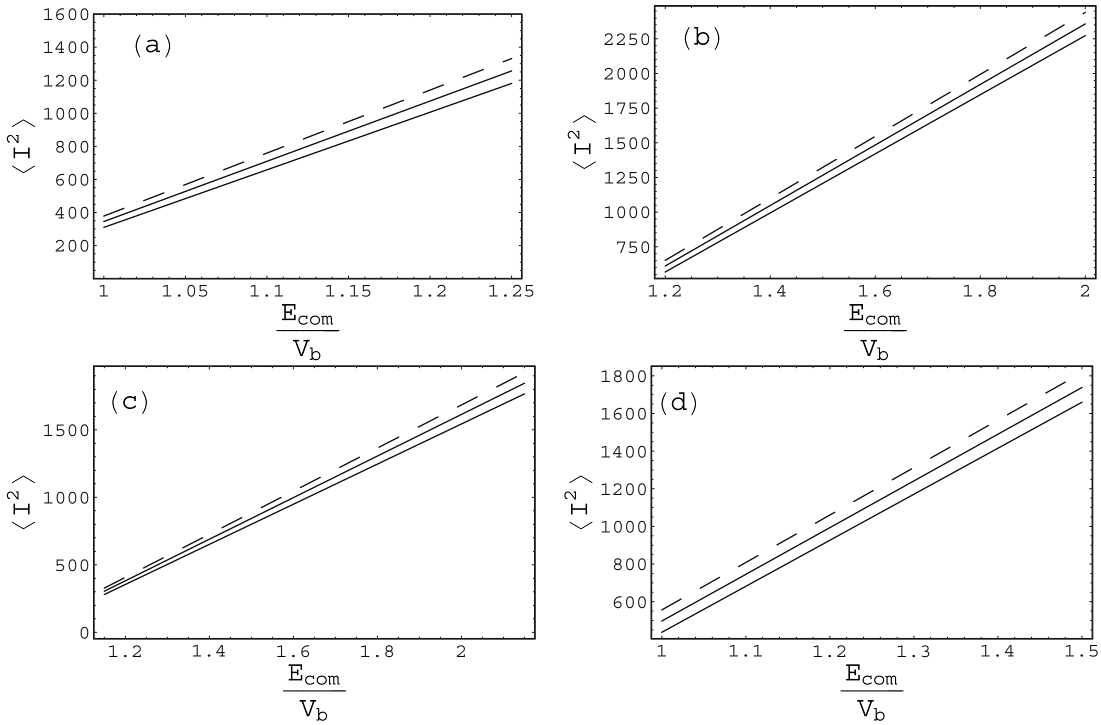

FIG. 1. Compound nucleus spin distributions for the systems that formed similar Cf isotopes. The dashed line shows spin distribution without correction of neutron emission, and the solid lines from top to bottom represent the spin distribution with neutron emission correction when the number of emitted neutrons is considered 1 and 2. (a) Spin distribution for the $^{16}O + ^{232}Th$ system. (b) Spin distribution for the $^{12}C + ^{236}U$ system. (c) Spin distribution for the $^{11}B + ^{237}Np$ system. (d) spin distribution for the $^{32}S + ^{208}Pb$ system.

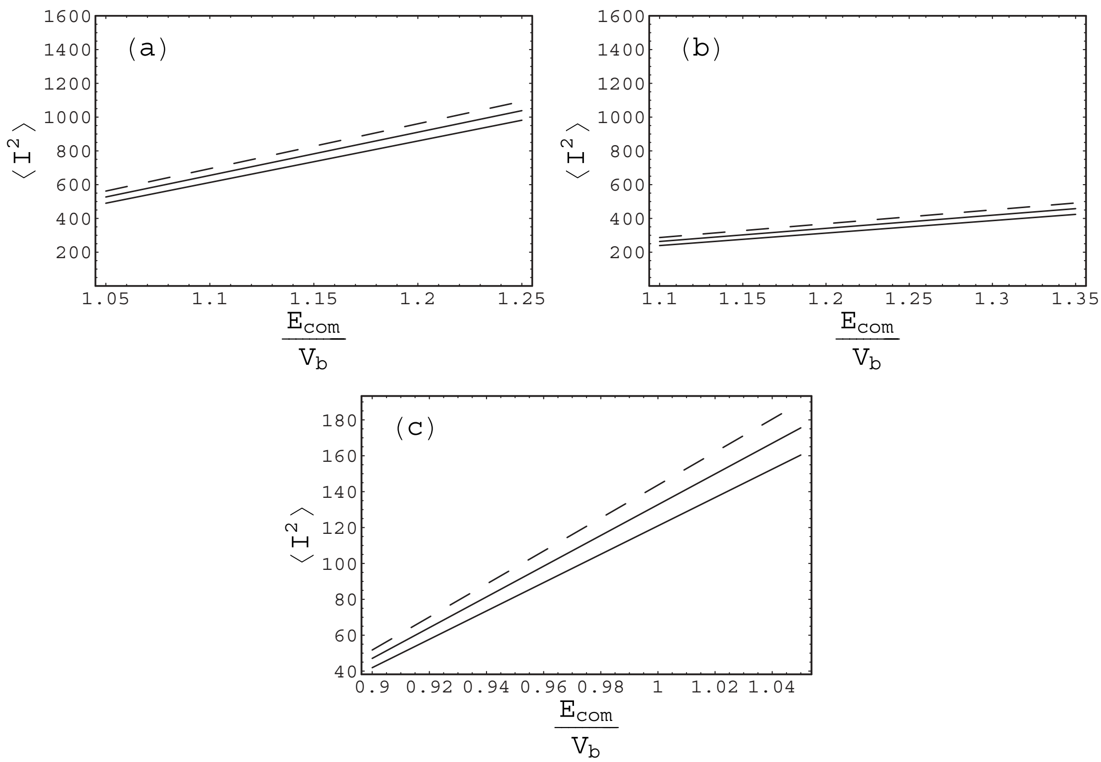

FIG. 2. Compound nucleus spin distributions for the systems that formed similar Bk isotopes. The dashed line shows spin distribution without correction of neutron emission, and the solid lines from top to bottom represent the spin distribution with neutron emission correction when the number of emitted neutrons is considered 1 and 2. (a) Spin distribution for the $^{14}N + ^{232}Th$ system. (b) Spin distribution for the $^{11}B + ^{235}U$ system. (c) Spin distribution for the $^{11}B + ^{238}U$ system.

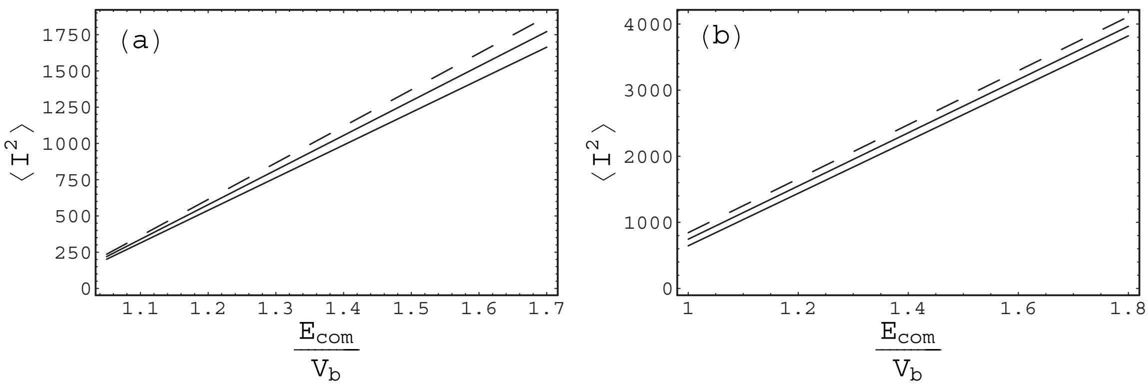

FIG. 3. Compound nucleus spin distributions for the systems that formed similar Cm isotopes. The dashed line shows spin distribution without correction of neutron emission, and the solid lines from top to bottom represent the spin distribution with neutron emission correction when the number of emitted neutrons is considered 1 and 2. (a) Spin distribution for the ^{12}C + ^{232}Th system. (b) Spin distribution for the ^{28}Si + ^{208}Pb system.

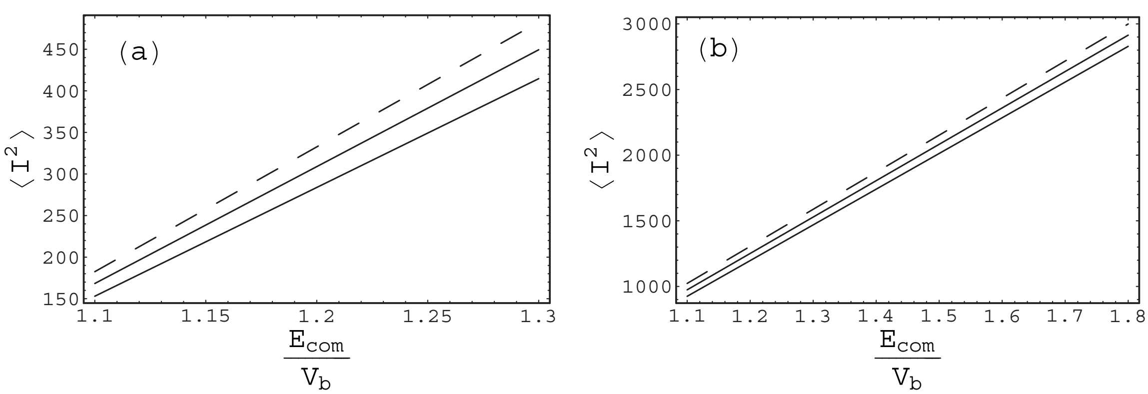

FIG. 4. Compound nucleus spin distributions for the systems that formed similar Pu isotopes. The dashed line shows spin distribution without correction of neutron emission, and the solid lines from top to bottom represent the spin distribution with neutron emission correction when the number of emitted neutrons is considered 1 and 2. (a) Spin distribution for the ^{9}Be + ^{232}Th system. (b) Spin distribution for the ^{24}Mg + ^{208}Pb system.

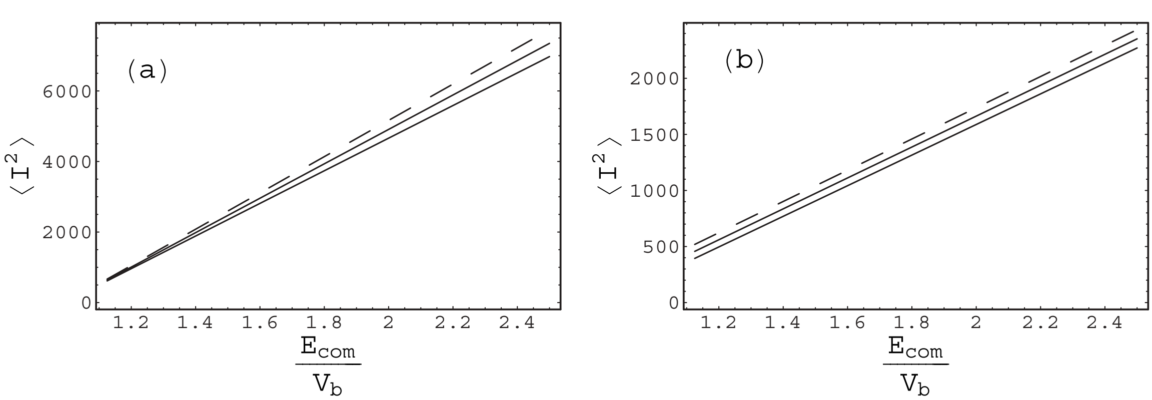

FIG. 5. Compound nucleus spin distributions for the systems that formed similar Pa isotopes. The dashed line shows spin distribution without correction of neutron emission, and the solid lines from top to bottom represent the spin distribution with neutron emission correction when the number of emitted neutrons is considered 1 and 2. (a) Spin distribution for the ^{16}O + ^{209}Bi system. (b) Spin distribution for the ^{19}F + ^{208}Pb system.

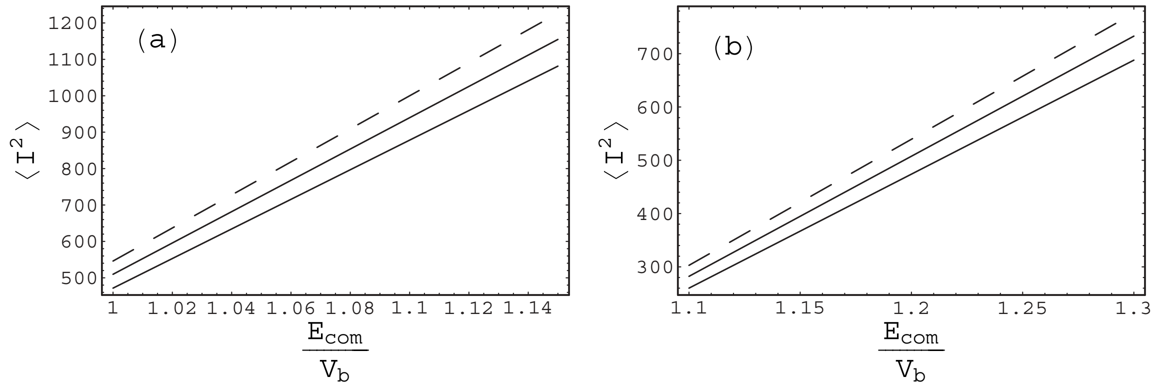

FIG. 6. Compound nucleus spin distributions for the systems that formed similar Es isotopes. The dashed line shows spin distribution without correction of neutron emission, and the solid lines from top to bottom represent the spin distribution with neutron emission correction when the number of emitted neutrons is considered 1 and 2. (a) Spin distribution for the ^{19}F + ^{232}Th system. (b) Spin distribution for the ^{12}C + ^{237}Np system.

nucleus spin distribution through comparing the experimental data for angular anisotropy of fission fragments [12] as well as the prediction of SSPSM. In this work, we have determined the values of compound nucleus spin distribution in terms of $\frac{E_{\text{c.m.}}}{V_b}$ for P + ^{197}Au and P + ^{209}Bi systems leading to ^{198}Hg and ^{210}Po compound nuclei, respectively. We take the relationships of $\langle I^2\rangle$ in terms of $\frac{E_{\text{c.m.}}}{V_b}$ as $\langle I^2\rangle = a_\nu \frac{E_{\text{c.m.}}}{V_b} + b_\nu$, where $\nu = 0, 1, 2$ denotes without considering the emission of neutron, emission of one neutron, emission of two neutrons, respectively. Table III shows a_ν and b_ν for these two systems.

Figure 10 shows the compound nucleus spin distribution determined by fission fragment angular distribution method with and without neutron emission correction for the P + ^{197}Au, and P + ^{209}Bi systems.

For the P + ^{209}Bi system, compound nucleus spin distribution is calculated by taking at most one neutron into account because the imaginary values of $\langle I^2\rangle$ is determined in terms of emitting two neutrons.

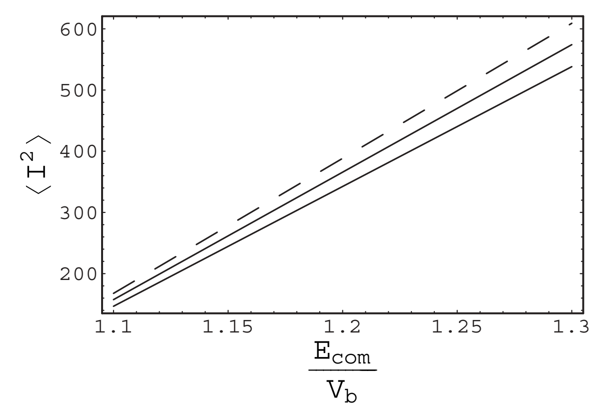

FIG. 7. Compound nucleus spin distributions for the ^{10}B + ^{232}Th system that formed ^{242}Am compound nucleus. The dashed line shows spin distribution without correction of neutron emission, and the solid lines from top to bottom represent the spin distribution with neutron emission correction when the number of emitted neutrons is considered 1 and 2.

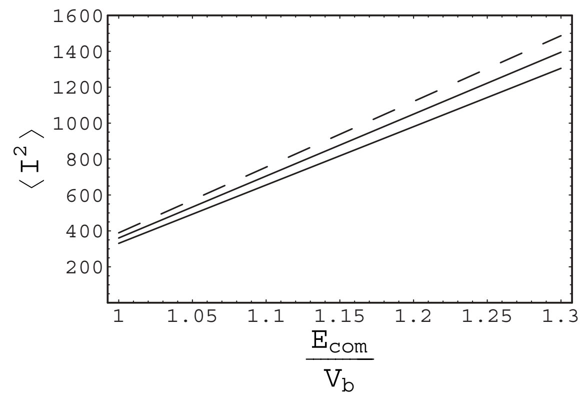

FIG. 8. Compound nucleus spin distributions for the ^{16}O + ^{208}Pb system that formed ^{224}Th compound nucleus. The dashed line shows spin distribution without correction of neutron emission, and the solid lines from top to bottom represent the spin distribution with neutron emission correction when the number of emitted neutrons is considered 1 and 2.

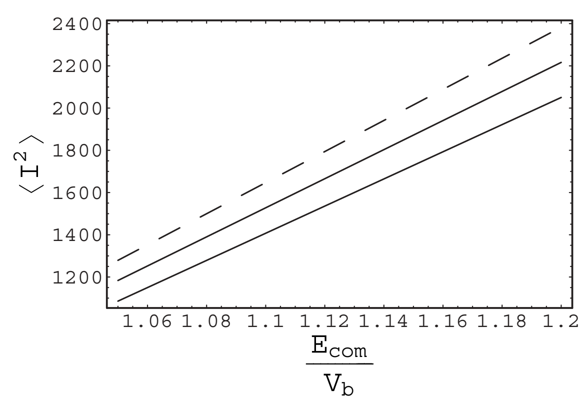

FIG. 9. Compound nucleus spin distributions for the ^{19}F + ^{197}Au system that formed ^{216}Ra compound nucleus. The dashed line shows spin distribution without correction of neutron emission, and the solid lines from top to bottom represent the spin distribution with neutron emission correction when the number of emitted neutrons is considered 1 and 2.

TABLE III. Coefficients of equation $\langle I^2 \rangle$ in terms of $\frac{E_{\text{c.m.}}}{V_b}$ without considering neutron emission and by considering the correction related to neutron emission.

Proton induced fission systems	$a_\circ$	$b_\circ$	a_1	b_1	a_2	b_2
P + ^{197}Au	49.43	−59.00	47.37	−62.65	52.80	−84.15
P + ^{209}Bi	20.44	−17.48	24.75	−31.63	–	–

IV. DETERMINATION OF $\langle I^2 \rangle$ USING QUANTUM-CLASSICAL RELATIONSHIPS

The maximum angular momentum transferred to the compound nucleus, I_{max}, was calculated according to the semiempirical formula [2]:

$$I_{\text{max}} = 0.155 r_\circ \left(A_i^{1/3} + A_t^{1/3}\right) \left[\frac{E_i A_i^2 A_t}{(A_i + A_t)^2}\right]^{1/2}, \qquad (5)$$

where A_i, A_t, E_i, and $r_\circ$ are the mass number of projectile, the mass number of target, the kinetic energy of projectile, and the radius constant, respectively. The maximum angular momentum $\langle I_{\text{max}} \rangle$ on the basis of quantum relationships is given by

$$I_{\text{max}} = \sqrt{2\mu r_b (E_i - V_b)}, \qquad (6)$$

where μ, r_b, and V_b are the reduced mass of projectile and target, the fusion barrier radius constant, and the fusion barrier height, respectively.

The mean-square angular momentum $\langle I^2 \rangle$ for the compound nucleus was set equal to $I_{\text{max}}^2/2$. From above, compound nucleus spin distribution $\langle I^2 \rangle$ can be approximated as

$$\langle I^2 \rangle = \frac{A_i^2 A_t}{2(A_i + A_t)^2} r_b^2 \left(A_i^{1/3} + A_t^{1/3}\right)^2 \left(1 + \frac{m_i}{m_t}\right) \times E_{\text{c.m.}} - \frac{A_i^2 A_t}{2(A_i + A_t)^2} r_b^2 \left(A_i^{1/3} + A_t^{1/3}\right)^2 V_b, \qquad (7)$$

where m_i and m_t are the mass of projectile and the mass of target, respectively.

V. COMPARISON AND DISCUSSION

In Fig. 11, the values of compound nucleus spin distribution obtained from quantum-classical relationship for the ^{16}O + ^{232}Th and ^{14}N + ^{232}Th systems are compared with those of the coupled channel technique [13,14] and with those of the Wong model [15], respectively. In Fig. 12, the values of compound nucleus spin distribution obtained from fission fragment angular distribution method for the ^{16}O + ^{232}Th and ^{16}O + ^{208}Pb systems by considering correction related to the average number of neutrons [6] are compared with those of coupled channel technique as well as the values of compound nucleus spin distribution obtained from the fission fragment distribution method for the ^{14}N + ^{232}Th system by considering the correction related to two emitted neutrons are compared with those of the Wong model.

As seen, the results obtained from angular distribution method are in good agreement with those of the coupled channel technique as well as the Wong model, however the values of $\langle I^2 \rangle$ determined by using classical-quantum relationships are not very precise.

VI. SUMMARY AND CONCLUSIONS

Calculation of the values of spin distributions using the experimental data for fission fragment angular distribution as well as the prediction of the statistical models is a novel method, which has been carried out in this work for the first time.

In this work, $\langle I^2 \rangle$ is calculated in terms of emitting one and two neutrons and compared with the case of ignoring the neutron emission. It was noted that the values of $\langle I^2 \rangle$, due to the neutron evaporation, decreases, usually less than 10%.

Considering the level density parameter as $a = \frac{A_{C.N.}}{8}, \frac{A_{C.N.}}{10}, \frac{A_{C.N.}}{11}$, rather than $a = \frac{A_{C.N.}}{9}$, the quantity for spin distribution of the compound nucleus varies at most by 6 to 7 %. Hence, this quantity is not sensitive to the level density parameter selected in the computation.

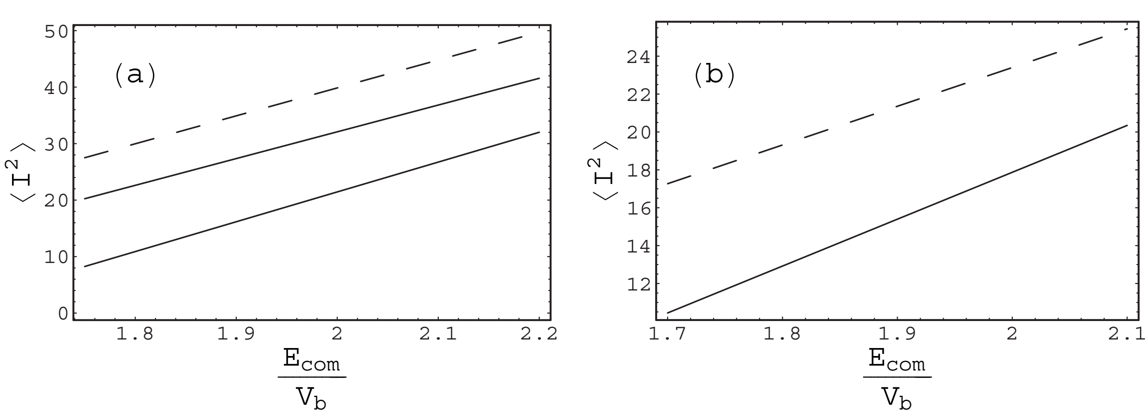

FIG. 10. Compound nucleus spin distributions for P + ^{197}Au, and P + ^{209}Bi systems. The dashed line shows spin distribution without correction of neutron emission, and the solid lines from top to bottom represent the spin distribution with neutron emission correction when the number of emitted neutrons is considered 1 and 2. (a) Spin distribution for the P + ^{197}Au system. (b) Spin distribution for the P + ^{209}Bi system.

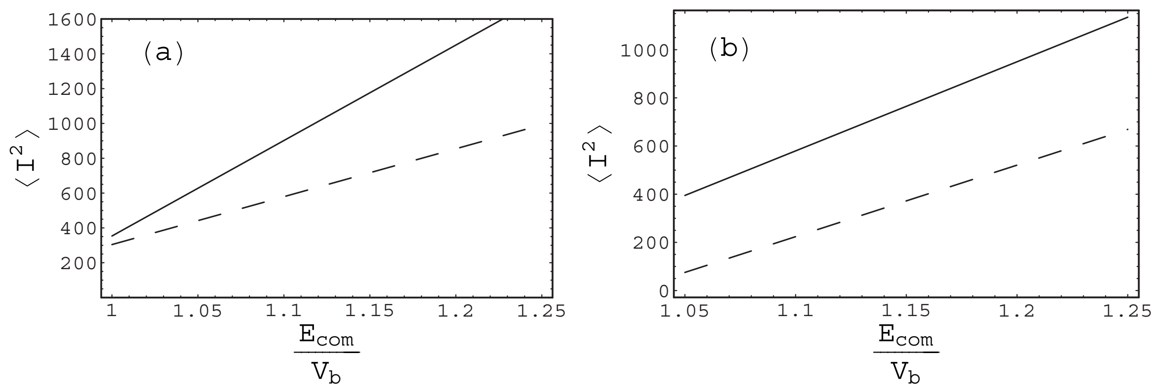

FIG. 11. (a) The comparison of $\langle I^2 \rangle$ obtained from the quantum-classical relationship (solid line) for the $^{16}O + {}^{232}Th$ system with those of the coupled channel technique (dashed line). (b) The comparison of $\langle I^2 \rangle$ obtained from quantum-classical relationship (solid line) for the $^{14}N + {}^{232}Th$ system with those of Wong model (dashed line).

In the second method, using quantum-classical relationships, an approximate formula for $\langle I^2 \rangle$ results which do not agree with previous ones was obtained.

The calculated values for $\langle I^2 \rangle$ by the fission fragment angular distribution method for the $^{16}O + {}^{232}Th$ and $^{16}O + {}^{208}Pb$ systems by considering the correction related to the average number of neutrons are compared with those of the coupled channels technique and for the $^{14}N + {}^{232}Th$ system by considering correction related to two emitted neutrons with those of the Wong model. Both of which were in agreement.

Overall, as experimental values of fission fragment angular distribution are used in this method, we can conclude that fission fragment angular distribution has been successful to calculate compound nucleus spin distribution.

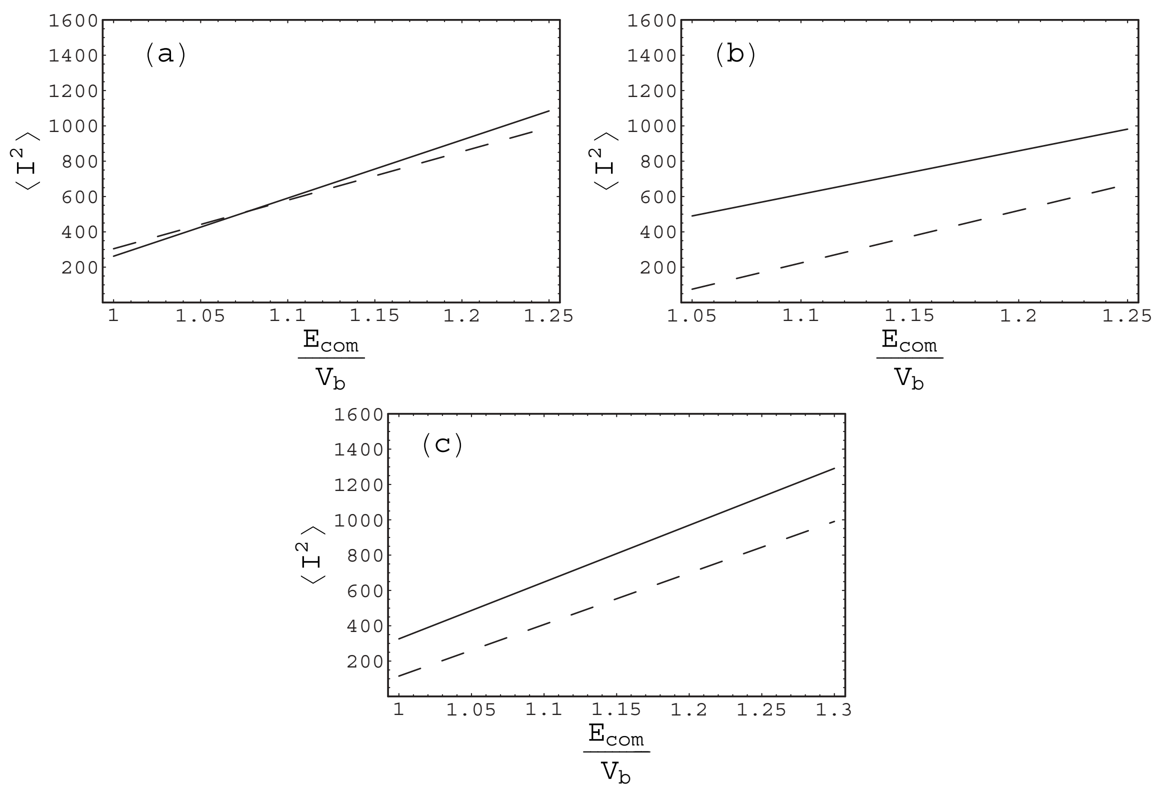

FIG. 12. (a) The comparison of $\langle I^2 \rangle$ obtained from fission fragment distribution method (solid line) for the $^{16}O + {}^{232}Th$ system by considering the correction related to the average number of emitted neutrons with those of the coupled channel technique (dashed line). (b) The comparison of $\langle I^2 \rangle$ obtained from the fission fragment distribution method (solid line) for the $^{14}N + {}^{232}Th$ system by considering the corrections related to two emitted neutrons with those of the Wong model (dashed line). (c) The comparison of $\langle I^2 \rangle$ obtained from the fission fragment distribution method (solid line) for the $^{16}O + {}^{208}Pb$ system by considering the corrections related to the average number of emitted neutron with those of the coupled channel technique (dashed line).

[1] R. Vandenbosch and J. R. Huizenga, *Nuclear Fission* (Academic Press, New York, 1973).
[2] M. G. Itkis, S. M. Lukyanov, V. N. Okolovich, Yu. E. Penionzhkevich, A. Ya. Rusanov, V. S. Salamatin, G. N. Smirenkin, and G. G. Chubaryan, Sov. J. Nucl. Phys. **52**(1), 15 (1990).
[3] S. D. Beizin, M. G. Itkis, I. A. Kamanev, S. I. Mulgin, V. N. Okolovich, and G. N. Smirenkin, Sov. J. Nucl. Phys. **43**, 883 (1986).
[4] S. Kailas, Phys. Rep. **284**, 381 (1997).
[5] S. Soheyli, H. Noshad, and I. Ziaian, IJMPE **17**, 1 (2008).
[6] R. K. Choudhury and S. S. Kapoor, PINSA **66A**, No. 6, 599 (2000).
[7] H. Zhang, Z. Liu, J. Xu, X. Qian, Y. Qiao, C. Lin, and K. Xu, Phys. Rev. C **49**, 926 (1994).
[8] S. Kailas, D. M. Nadkarni, A. Chatterjee, A. Saxena, S. S. Kapoor, R. Vandenbosch, J. P. Lestone, J. F. Liang, D. J. Prindle, A. A. Sonzogni, and J. D. Bierman, Phys. Rev. C **59**, 2580 (1999).
[9] R. Bahera, S. Kailas, K. Mahata, A. Chatterjee, P. Basu, S. Roy, M. Satpathy, and S. K. Datta, Nucl. Phys. A **734**, 249 (2004).
[10] R. Tripathi, K. Surdashan, S. Sodaye, A. V. R. Reddy, K. Mahata, and A. Goswami, Phys. Rev. C **71**, 044616 (2005).
[11] Z. Huanqiao, L. Zuhua, X. Jincheng, Q. Xing, C. Shaolin, and L. Lixing, Chinese Phys. Lett. **9**, 297 (1992).
[12] S. Soheyli, H. Noshad, and M. Lamehi-Rachti, IJMPA **22**, 1027 (2007).
[13] C. H. Dasso, S. Landowne, and A. Winther, Nucl. Phys. A **405**, 381 (1983); I. J. Thompson, M. A. Nagarajan, J. S. Lilley, and M. J. Smithson, *ibid.* **505**, 84 (1989).
[14] R. Vandenbosch, Annu. Rev. Nucl. Part. Sci. **42**, 447 (1992).
[15] C. Y. Wong, Phys. Rev. Lett. **31**, 766 (1973).